Biophysical Journal, Volume 99

**Supporting Material**

# Shaping a morphogen gradient for positional precision

Feng He, Timothy E Saunders, Ying Wen, David Cheung, Renjie Jiao, Pieter Rein ten Wolde, Martin Howard, and Jun Ma

# Shaping a Morphogen Gradient for Positional Precision: Supplementary Material

Feng He, Timothy Saunders,Ying Wen, David Cheung, Renjie Jiao, Pieter Rein ten Wolde, Martin Howard and Jun Ma

## S1 Analysis of Wildtype Embryos

### S1.1 Curve Fitting wt Bcd Profiles

We describe the curve fitting procedure for the observed mean intensity profiles before presenting a more detailed analysis of the observed fluctuations. Here, all results are in terms of distances scaled by embryo length, with results for absolute distances given later, see Section S5.

Within the region $x_1/L = 0.19 < x/L < x_2/L = 0.49$, the observed intensity profiles of all 28 wt embryos are well fit by an exponential decay. For $x > x_2$, the observed intensities are close to the background level and an exponential profile can no longer be confidently fit. In the region $x < x_1$, the point from where exponential profiles are a good fit to the observed profiles varies significantly between embryos ($x_1^{min}/L = 0.03$, $x_1^{max}/L = 0.19$). To ensure that we are measuring within the region well fitted by exponentials, for all embryos we only consider data between a lower limit of $x_1/L = 0.19$ and an upper limit $x_2/L = 0.49$.

The embryos are separated into 'early' and 'late' data sets so that embryos at similar developmental stages are compared, see the Materials and Methods section below. The profiles are subject to fluctuations from embryo-to-embryo as well as internal noise and background variations. To reduce the effect of these fluctuations we perform averaging to find the mean observed Bcd intensity as a function of position for each data set separately. Strictly, the arithmetic mean of exponentials is not an exponential. However, an exponential fit to the average profile was found to be excellent ($r^2 > 0.994$). An alternative approach using median parameter values [1] made little difference to our analysis. The average profile is then fitted to

$$B = B_1 e^{-y/\Lambda} . \tag{S1}$$

Here, $\Lambda = \lambda/L$ where $\lambda$ is the characteristic decay length of the exponential profile with $y = x/L - x_1/L$ and $B_1$ the intensity at $y = 0$. The values $B_1$ and $\Lambda$ for the average profile are found using a least-squares analysis, see values shown in Table S1. Note that the form of Eq. S1 makes no assumptions about the underlying dynamics of gradient formation. In our experiments we find, after background subtraction, that there is still a non-zero Bcd intensity in the posterior region of the embryo. We can fit the experimentally observed intensity in a wider region of the embryo by considering $B = B_1 e^{-y/\Lambda} + b$, where $b$ is a constant. However, we find that such an approach makes little difference to our results within the region $x_1 < x < x_2$ and hence we set $b = 0$ throughout.

## S1.2 Parameter Fitting of Bcd Profile Fluctuations in wt Embryos

The fluctuations in intensity and positional information of the observed wt Bcd profiles are shown in Fig. 2 in the main paper. Here, we discuss our methodology for fitting these experimentally observed fluctuations. First, we demonstrate that each parameter in Eq. (2) in the main paper is important for fitting the observed intensity fluctuations at different positions in the embryo and hence that we are not over-fitting the data. We then discuss further checks to ensure our fits are realistic.

$\delta B_1^{ind}$: Fluctuations in $B_1^{ind}$ are constrained by the requirement to reproduce the observed values of $\delta B/B$ and $W_{Bcd}/L$ near $x/L = 0.2$. Altering other parameters to fit $\delta B/B$ near $x/L = 0.2$ results in inadequate fits elsewhere in the embryo. As an example, if we increase the effects of internal noise to match the observed fluctuations near $x/L = 0.2$ the predicted fluctuations at $x/L \sim 0.5$ would be too large.

$\delta\Lambda$ and $\alpha_1$: The only functional part of Eq. (2) in the main paper that can decrease for $x/L > 0.19$ is the term $((y/\Lambda+\alpha_1)\delta\Lambda/\Lambda)^2$, where $\alpha_1 < 0$ since $\Lambda$ and $B_1$ are anti-correlated, see Fig. S1B. Therefore, $\alpha_1$ and $\delta\Lambda/\Lambda$ are constrained by the observed minimum in $\delta B/B$ and $W_{Bcd}/L$ close to $x/L = 0.3$.

$V$: $V$ is kept constant in all fits, for both wt and *nej* embryos. Therefore, the value of $V$ is heavily constrained by the requirement to fit 8 data sets (Fig. 2 in the main paper, for both wt embryos and *nej* embryos). In particular, we find that $V$ is constrained by the requirement to fit the observed fluctuations near mid-embryo.

Measurement noise: $\delta B_{meas}/B$ is fixed by experiment and is not fitted. In Fig. S1A we show the measured error from background, imaging and processing noise (for a more complete discussion see He et al. [2]) along with the fit to $\delta B_{meas} = a + by$. The relative imaging noise is roughly constant for $x/L < 0.5$ whilst the relative processing noise is largest near the anterior and gradually decreases towards the posterior. Conversely, the relative error in background subtraction increases at larger $x/L$.

In Fig. S3A,C, we demonstrate the fits to the observed intensity and position variations in the Bcd gradient for late wt embryos, showing the individual contributions that make up Eq. (2) in the main paper. We see that each contribution (excluding the measurement noise which is measured rather than fitted) is necessary for correct fitting of the data. Therefore, our parameters are properly constrained and we are not over-fitting the data. Complete parameter values are given in Table S2.

To further test our fits, we compared the values of $\delta B_1^{ind}/B_1^{ind}$ and $\delta\Lambda/\Lambda$ found from our fitting to the overall observed experimental fluctuations with those derived from individual embryos, see Fig. S1B. In Fig. S1B, the gradients of the solid lines depend on the $\alpha_1$ values found previously, and are an excellent fit to the data. Finally, it is also informative to plot the relative intensity fluctuations (coefficient of variation), shown in Fig. S4. We see that the relative fluctuations increase toward the posterior, as expected.

# S2 Analysis of *nej* Embryos

## S2.1 Curve Fitting Bcd Profiles in *nej* Embryos

The intensity profiles of the *nej* embryos are very well fitted by an algebraically decaying function in the region $x_1 < x < x_2$, see Figs. 1A and 1B in the main paper. We consider

the form (where $y = x/L - x_1/L$ and $y_0 = x_0/L + x_1/L$)

$$B = \frac{a_n}{(y + y_0)^n}\,. \tag{S2}$$

The constant $n$ is determined by fitting the average Bcd profile in *nej* embryos in the range $0.0 < y < 0.3$ and finding the median value of $n$ such that the quality of the fit $r^2 > 0.995$ (in this region, all the fitted parameter sets $\{a_n,\ y_0,\ n\}$ are excellent matches to the data and it is not meaningful to distinguish between them), giving $n = 2.7 \pm 1.2$, see Fig. S2A. Fitting each Bcd profile individually in *nej* embryos and using the median parameter values yielded very similar results. We also confirmed that varying $n$ within the appropriate range does not significantly alter our results ($n = 2$ and $n = 3.5$ tested). The parameters $a_n$ and $y_0$ are deduced from a least-squares analysis, with values given in Table S3.

We compare the best algebraic fit to the Bcd intensity profile in *nej* embryos with the corresponding best exponential fit using Eq. S1. In Fig. S2B we see that the exponential is clearly sub-optimal when compared to algebraic curve fitting. The inset to Fig. S2B highlights the relative quality of the fit throughout the region of interest. However, other more complex functional forms, such as $B = B_2 e^{-y/\Lambda_2} + b$ and $B = B_3(e^{-y/\Lambda_3} + e^{-y/\Lambda_4})$, also fit the data well. Henceforth, we will use Eq. S2 in our dissection of the fluctuations, although using these other more complex fits does not change our results. In particular, we have repeated the analysis outlined in the paper using $B = B_3 e^{-y/\Lambda_2} + b$, where we find similar results for the precision of the Bcd gradient.

## S2.2 Embryo-to-Embryo Fluctuations

Our data clearly reveals a strong correlation between $a_n$ and $y_0$ which must be taken into account, see Fig. S2C. Following a similar procedure to the $B_1 - \Lambda$ correlation, we consider $a_n = a_n^{ind} g(y_0)$, where we assume that the variables are separable. To leading order, the relative intensity fluctuations due to external embryo-to-embryo variations in $a_n$ and $y_0$ are

$$\frac{\delta B_{ext}}{B} = \left[ \left( \frac{\delta a_n^{ind}}{a_n^{ind}} \right)^2 + \left( \left[ \alpha_2 - \frac{n y_0}{y + y_0} \right] \frac{\delta y_0}{y_0} \right)^2 \right]^{1/2}, \tag{S3}$$

where $\alpha_2 = y_0 g'(y_0)/g(y_0)$ is an additional fitting parameter.

## S2.3 Internal Fluctuations

The relative fluctuations from internal stochastic processes for *nej* embryos can be handled in a similar way to the wt case. Substituting Eq. S2 into $\delta B_{int}/B = 1/\sqrt{VB}$ [3], we find

$$\frac{\delta B_{int}}{B} = \frac{(y + y_0)^{n/2}}{\sqrt{V a_n}}\,. \tag{S4}$$

## S2.4 Measurement Fluctuations

The relative error in the measurement of the background is larger in *nej* embryos due to the smaller absolute intensities. From the experimental data, we see that once fluctuations in the measurement of the background level and measurement errors due to imaging/processing noise are accounted for, $\delta B_{meas}/B \approx cy$ in the region $0 < y < 0.3$, where $c = 0.16 \pm 0.05$, see Fig. S1A.

## S2.5 Combining Sources of Error

As in the wt analysis, we have now separated the sources of error into four independent contributions, and hence the overall relative intensity fluctuations for *nej* embryos are given by

$$\left(\frac{\delta B}{B}\right)_{nej} = \left[\left(\frac{\delta a_n^{ind}}{a_n^{ind}}\right)^2 + \left(\left[\alpha_2 - \frac{n y_0}{y + y_0}\right]\frac{\delta y_0}{y_0}\right)^2 + (cy)^2 + \frac{(y + y_0)^n}{V a_n}\right]^{1/2}. \tag{S5}$$

The corresponding relative positional error can then be found using Eq. 3 in the main paper.

## S2.6 Parameter Fitting of Bcd Profile Fluctuations in *nej* Embryos

The relative Bcd intensity fluctuations and positional error are shown in Fig. S3B and Fig. S3D respectively, with the contributions from each source of error in Eq. S5 plotted separately (for late *nej* embryos). $\delta a_n^{ind}/a_n^{ind}$ is needed to get the correct values of $\delta B/B$ and $W_{Bcd}/L$ near $x/L = 0.2$ (similar to the constraint on $\delta B_1^{ind}/B_1^{ind}$ for the wt). $\alpha_2$ and $\delta y_0/y_0$ are constrained by the observed minimum in $\delta B/B$ close to $x/L = 0.25$. $\delta B_{meas}/B$ is fixed by experiment [2] and is not fitted, see Fig. S1A. Therefore, our parameters are properly constrained and we are not over-fitting the data. The parameters used to fit the observed experimental fluctuations are given in Table S4. Similar to the wt case, we demonstrate in Fig. S2C that the fitted values of $\alpha_2$ are consistent with the data from individual embryos. Finally, we show the relative intensity fluctuations for *nej* embryos in Fig. S4. As with wt embryos, we see that the relative fluctuations increase toward the posterior. Furthermore, *nej* embryos have larger relative fluctuations than wt embryos throughout the region $x_1 < x < x_2$, as expected.

# S3 Other Sources of Fluctuations

We have neglected other sources of noise in our analysis, such as fluctuations in the downstream events after Bcd binding to its DNA target sites. Detailed analysis of the Bcd-*hb* circuit suggests that such downstream noise is less important in determining Hb precision [4] and we therefore treat the time/spatial averaging processes as ideal. It has also been suggested that one-dimensional sliding of Bcd along DNA could reduce error, although a theoretical study has predicted that the fluctuations related to such motion will be similar to fully three-dimensional diffusion [5]. The Hb profile itself is subject to both measurement and internal fluctuations which could be possible sources of additional errors. Following the procedures outlined for analysing the fluctuations in the Bcd profiles, we can perform a similar analysis for the Hb profiles. However, comparing the relative magnitude of these fluctuations with those in Bcd, we see that they are typically between 5 and 20 times smaller around the threshold position and hence we neglect them. The reduced effect of Hb fluctuations is due to the steepness of the Hb profile around the threshold position.

# S4 Orthodenticle Precision

As detailed in the main text, we make several assumptions in our calculation of Otd boundary precision. We emphasise that, even if these assumptions are only approximately correct, our prediction that wt and *nej* embryos have similar Otd boundary precision (i.e. $W_{Otd}^{wt} \approx W_{Otd}^{nej}$) will still hold, though the predicted value for that precision will be altered. For example, if the averaging time is only 5 minutes then (for the early subgroup) $W_{Otd}^{wt}/W_{Otd}^{nej} \approx 0.81$ and if the averaging time is 20 minutes then $W_{Otd}^{wt}/W_{Otd}^{nej} \approx 0.86$. This is due to the wt and *nej* profiles having similar steepnesses, and the effects of density fluctuations being approximately equal, at the Otd boundary. This contrasts with the Hb boundary, where we predict that wt embryos will define position more precisely than *nej* embryos, as found experimentally. As detailed in the main paper, these results support our conclusion that it is the different profile shape that is primarily responsible for the reduced Hb boundary precision in *nej* embryos, and not other defects due to the absence of dCBP. Finally, as with Hb, the Otd profile is itself subject to both measurement and internal fluctuations which could be possible sources of additional errors. Again, we find that such fluctuations are small compared to those in Bcd (due to the Otd profile being steeper at the threshold position), and we therefore neglect them.

# S5 Absolute Positional Information

All of the above analysis can be repeated using absolute length scales, rather than length scaled by the total embryo length. In general, in agreement with [2], we find that the measured fluctuations using absolute lengths are now larger in the region $x_1 = 105\mu m$ ($x_1/L \approx 0.19$) to $x_2 = 270\mu m$ ($x_2/L \approx 0.49$). Our theory still correctly fits the observed data, where unscaled variables such as $\lambda = L\Lambda$ and $x_0 + x_1 = Ly_0$ are used, since our general analytical methodology is not dependent upon using scaled variables. However, without scaling there is increased positional error. We show in Fig. S5 equivalent fits to the scaled case shown in Fig. 2A-D in the main paper, where the axes in Fig. S5 are scaled by the average embryo length $\langle L \rangle$ to facilitate comparison with the scaled analysis. Typically, the values for $\delta\lambda/\lambda$, $\delta x_0/x_0$ etc. are between 10-50% larger than their scaled equivalents (see Table S6).

We can also analyse the precision of the Hb boundary in terms of absolute position. Applying a similar analysis to Sections S1 and S2, we find $W_{Bcd}/\langle L \rangle = 0.021 \pm 0.013$ (early, wt), $W_{Bcd}/\langle L \rangle = 0.038 \pm 0.020$ (late, wt), $W_{Bcd}/\langle L \rangle = 0.034 \pm 0.018$ (early, *nej* embryos), and $W_{Bcd}/\langle L \rangle = 0.048 \pm 0.029$ (late, *nej* embryos). It is clear that the positional information is less precise, consistent with other results showing that scaling is important for correct Hb boundary positioning [1, 2, 6].

# S6 Materials and Methods

**Embryo staining and intensity measurements.** All embryos described in this report were collected at $25^oC$. Females with *nej*[1] germline clones were generated as reported [7–9]. Embryo staining with anti-Bcd and anti-Hb antibodies, high-resolution digital imaging, raw intensity measurement, background subtraction, and calculation of background and measurement noises were all performed as described [2]. For our antibody staining data described in this work, we used the same criteria for selecting embryos at the early nuclear

cycle 14 as before [2], namely, all embryos had a nuclear height:width ratio of $\sim 1.3-1.7:1$ and a normalized posterior Hb intensity $< 0.5$; the posterior Hb expression, similar to the Hb PS4 stripe, is driven by another *hb* enhancer that is distinct from the Bcd-responsive enhancer [10]. To improve our measurements and facilitate theoretical calculations, the selected wt ($w^{1118}$) and *nej* embryos were further split into early (normalized posterior Hb intensity $< 0.25$) and late subgroups (normalized posterior Hb intensity $\geq 0.25$); all quantitative studies described in this report analyze separately the subgroup data unless stated otherwise. For our quantification of raw Bcd and Hb intensity measurements, we estimate a measuring volume of $\sim 200\mu m^3$ (a cylinder with $\sim 6\mu m$ diameter and $\sim 6\mu m$ height), which roughly corresponds to the volume of a nucleus at the developmental stage of our experimental embryos. The expression boundary of a *hb-lacZ* reporter gene (*T306* [11]) driven by the Bcd-dependent *hb* enhancer in early nuclear cycle 14 was determined using fluorescent in situ hybridization [12] and a quantification method as described [6]; with $n = 18$ the number of embryos. The expression profile of Otd in wt ($n = 39$) and *nej* ($n = 38$) embryos at early nuclear cycle 14 was determined in co-staining experiments with guinea pig anti-Otd [13] and rat anti-Hb [14] primary antibodies and secondary antibodies (Molecular Probes) that were conjugated to, respectively, Alexa-448 and Alexa-555. The intensity data extracted from Otd-Hb co-stained embryos at early nuclear cycle 14 were not further split into early and late subgroups as for the Bcd-Hb co-stained embryos since an additional criterion (that embryos must have detectable and reliable intensity signals for both Otd and Hb) had to be used in selecting embryos for our analysis. All other experimental and analytical procedures in the Otd-Hb co-staining analysis were as described previously [2].

**Discussion on the use of raw Bcd intensities.** In this study, we used raw Bcd intensities to avoid measurement distortions caused by intensity normalizations as discussed previously [2]. The following two findings suggest that the raw Bcd intensities detected in our experiments are sufficiently accurate without the need for further normalizations, except proper background subtraction. First, wt Bcd profiles measured as raw intensities exhibited a similar degree of embryo-to-embryo reproducibility as the profiles measured by live-imaging studies [2, 15]. Second, raw Bcd intensity noise measured among a group of wt embryos was comparable to raw Bcd intensity noise measured between neighboring nuclei in single embryos [2].

# References


[1] Manu, S. Surkova, A. V. Spirov, V. V. Gursky, H. Janssens, A. R. Kim, O. Radulescu, C. E. Vanario-Alonso, D. H. Sharp, M. Samsonova, and J. Reinitz, 2009. Canalization of gene expression in the *Drosophila* blastoderm by gap gene cross regulation. *PLoS Biol.* 7:e1000049.

[2] He, F., Y. Wen, J. Deng, X. Lin, L. J. Lu, R. Jiao, and J. Ma, 2008. Probing intrinsic properties of a robust morphogen gradient in *Drosophila*. *Dev. Cell* 15:558–567.

[3] Tostevin, F., P. R. ten Wolde, and M. Howard, 2007. Fundamental limits to position determination by concentration gradients. *PLoS Comp. Biol.* 3:763–771.

[4] Tkačik, G., T. Gregor, and W. Bialek, 2008. The Role of Input Noise in Transcription Regulation. *PLoS One* 3:e2774.

[5] Tkačik, G., and W. Bialek, 2009. Diffusion, dimensionality and noise in transcription regulation. *Phys. Rev. E* 79:051901.

[6] Houchmandzadeh, B., E. Wieschaus, and S. Leibler, 2002. Establishment of developmental precision and proportions in the early *Drosophila* embryo. *Nature* 415:798–802.

[7] Akimaru, H., Y. Chen, P. Dai, D. X. Hou, M. Nonaka, S. M. Smolik, S. Armstrong, R. H. Goodman, and S. Ishii, 1997. *Drosophila* CBP is a co-activator of cubitus interruptus in hedgehog signalling. *Nature* 386:735–738.

[8] Akimaru, H., D. X. Hou, and S. Ishii, 1997. *Drosophila* CBP is required for dorsal-dependent twist gene expression. *Nat. Genet.* 17:211–214.

[9] Lilja, T., H. Aihara, M. Stabell, Y. Nibu, and M. Mannervik, 2007. The acetyltransferase activity of *Drosophila* CBP is dispensable for regulation of the Dpp pathway in the early embryo. *Dev. Biol.* 305:650–658.

[10] Margolis, J. S., M. L. Borowsky, E. Steingrimsson, C. W. Shim, J. A. Lengyel, and J. W. Posakony, 1995. Posterior stripe expression of hunchback is driven from two promoters by a common enhancer element. *Development* 121:3067–3077.

[11] Driever, W., F. Thoma, and C. Nüsslein-Volhard, 1989. Determination of spatial domains of zygotic gene expression in the *Drosophila* embryo by the affinity of binding site for the bicoid morphogen. *Nature* 340:363–367.

[12] Kosman, D., C. M. Mizutani, D. Lemons, W. G. Cox, W. McGinnis, and E. Bier, 2004. Multiplex detection of RNA expression in *Drosophila* embryos. *Science* 305:846.

[13] Xie, B., M. Charlton-Perkins, E. McDonald, B. Gebelein, and T. Cook, 2007. Senseless functions as a molecular switch for color photoreceptor differentiation in *Drosophila*. *Development* 134:4243–4253.

[14] Kosman, D., S. Small, and J. Reinitz, 1998. Rapid preparation of a panel of polyclonal antibodies to *Drosophila* segmentation proteins. *Dev. Genes Evol.* 208:290–294.

[15] Gregor, T., E. F. Wieschaus, A. P. McGregor, W. Bialek, and D. W. Tank, 2007. Stability and nuclear dynamics of the Bicoid morphogen gradient. *Cell* 130:141–152.

[16] Saunders, T. E., and M. Howard, 2009. Morphogen profiles can be optimized to buffer against noise. *Phys. Rev. E* 80:041902.

[17] Gregor, T., D. W. Tank, E. F. Wieschaus, and W. Bialek, 2007. Probing the limits to positional information. *Cell* 130:153–164.

[18] Crauk, O., and N. Dostatni, 2005. Bicoid determines sharp and precise target gene expression in the *Drosophila* embryo. *Curr. Biol.* 15:1888–1898.

[19] Bergmann, S., O. Sandler, H. Sberro, S. Shnider, E. Schejter, B.-Z. Shilo, and N. Barkai, 2007. Pre-steady-state decoding of the Bicoid morphogen gradient. *PLoS Biol.* 5:e46.

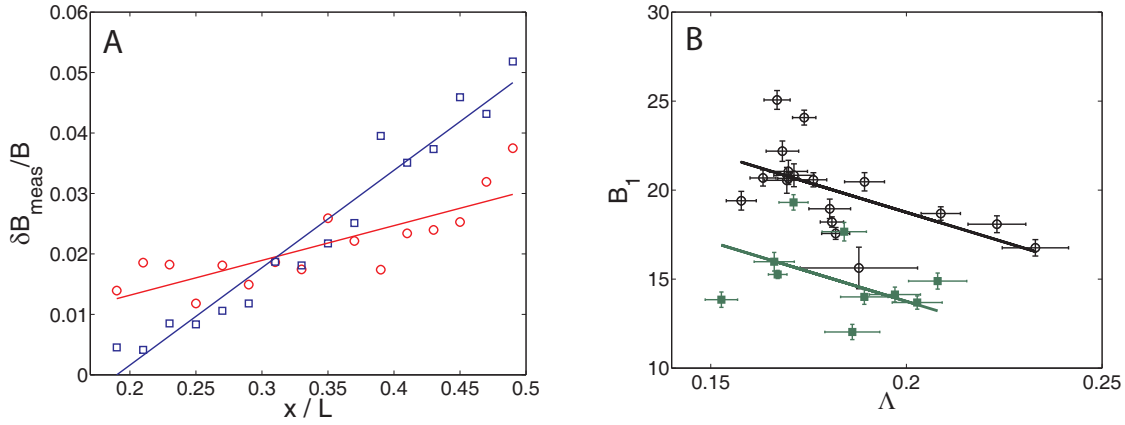


Figure S1: **Experimental error and $B_1 - \Lambda$ correlations**. **A**: $\delta B_{meas}/B$ against $x/L$. Red circles denote wt and blue squares denote *nej* embryos. There is no separation into early and late subgroups. Error bars omitted for clarity but are typically on the order of $\pm 0.02$ for both wt and *nej* embryos. $\delta B_{meas}/B$ includes measured imaging and processing noise from the experiments as well as background error. **B**: Correlation between $B_1$ (in arbitrary units) and $\Lambda$ for early (black $\circ$) and late (green $\blacksquare$) time data sets. Black and green lines derived from the values used to fit the observed Bcd intensity fluctuations/positional error at early and late times respectively.

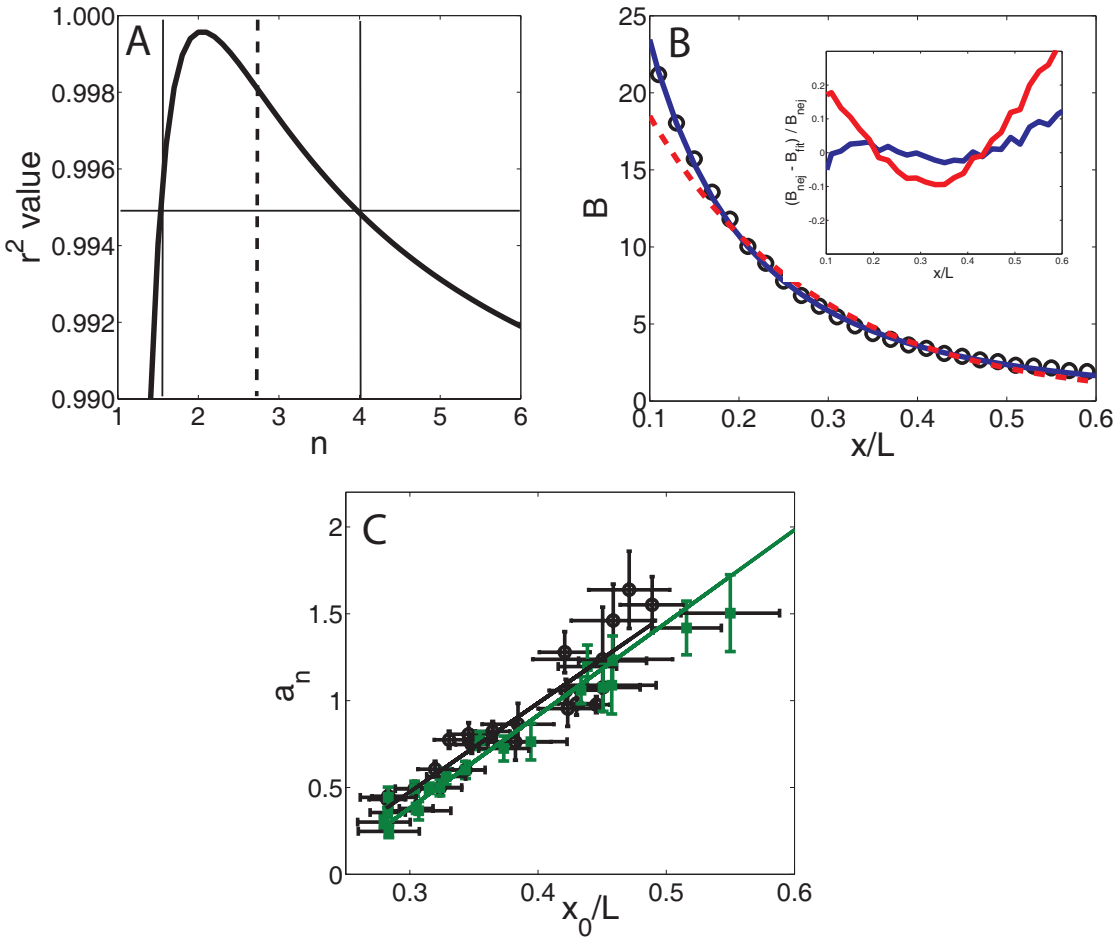


Figure S2: **Fitting *nej* embryos and $a_n - y_0$ correlations**. **A**: Quality of fit to the average Bcd intensity profile in *nej* embryos for varying $n$. Full vertical lines delineate the region where $r^2 > 0.995$, with $n = 2.7$ being the median value within this range (denoted by dashed line). **B**: Fitting the Bcd intensity profile in *nej* embryos (at early times) with algebraic (blue line) and exponential (red line) profiles. $B$ has arbitrary units. Inset: relative difference $(B_{nej} - B_{fit})/B_{nej}$ against $x/L$, where $B_{nej}$ is the average experimental Bcd intensity in *nej* embryos at position $x/L$ and $B_{fit}$ corresponds to the algebraic and exponential 'best fits' to the data at $x/L$. **C**: Correlation between $a_n$ (in arbitrary units) and $x_0/L$ for early (black ∘) and late (green ■) time data sets. Black and green lines derived from the values used to fit the observed Bcd intensity fluctuations/positional error in *nej* embryos at early and late times respectively.

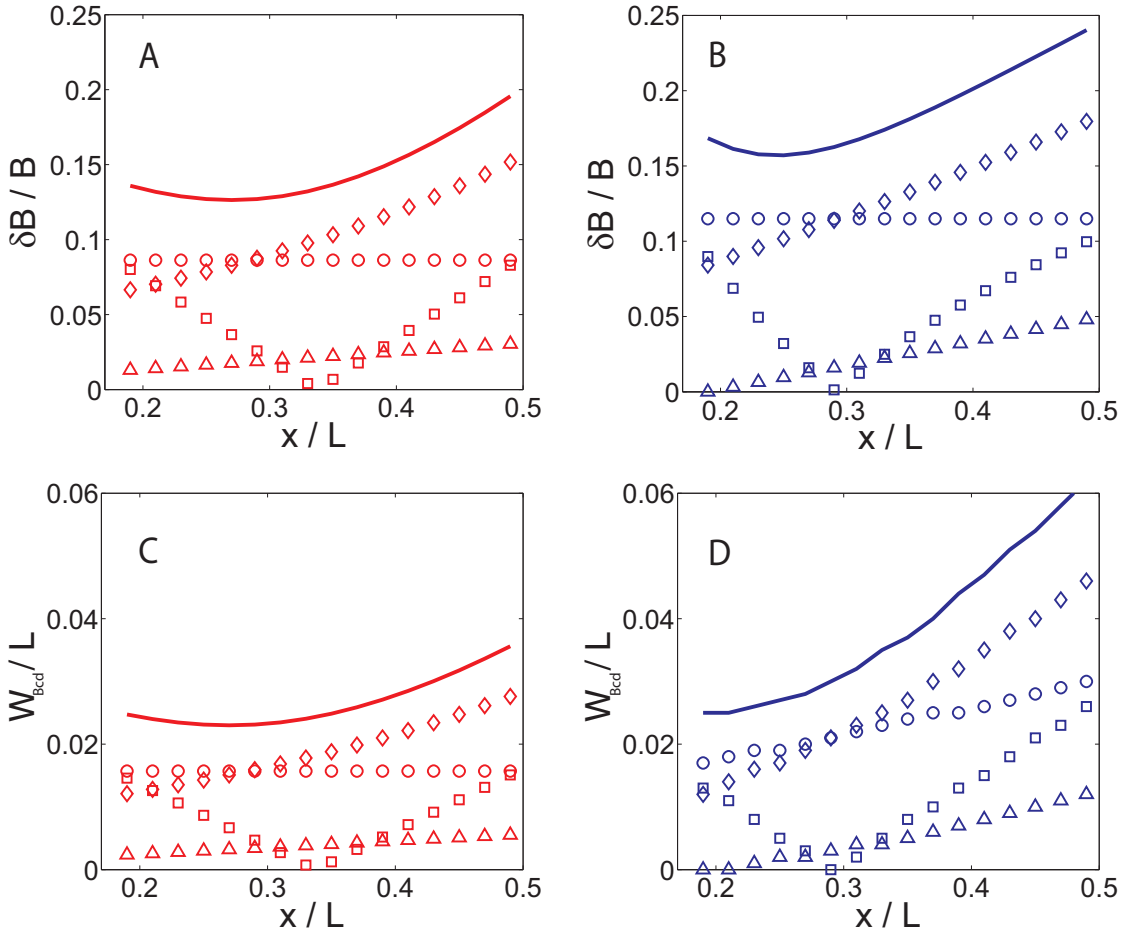


Figure S3: **Individual contributions to the observed fluctuations**. All results shown are for the late-time data sets. **A**: Contributions to relative Bcd intensity fluctuations in wt embryos: $\delta B_1^{ind}/B_1^{ind}$ ($\circ$); $\delta\Lambda/\Lambda$ ($\square$); $\delta B_{meas}/B$ ($\triangle$); and $\delta B_{int}/B$ ($\diamond$). **B**: Contributions to relative Bcd intensity fluctuations in *nej* embryos: $\delta a_n^{ind}/a_n^{ind}$ ($\circ$); $\delta y_0/y_0$ ($\square$); $\delta B_{meas}/B$ ($\triangle$); and $\delta B_{int}/B$ ($\diamond$). **C**: Contributions to positional error in wt embryos. Bcd intensity fluctuations for wt embryos are converted into positional error using Eq. 3 in the main paper. Symbols as **A**. **D**: Contributions to positional error in *nej* embryos. Bcd intensity fluctuations for *nej* embryos are converted into positional error using Eq. 3 in the main paper. Symbols as **B**.
Total relative fluctuations/positional error denoted by solid line.

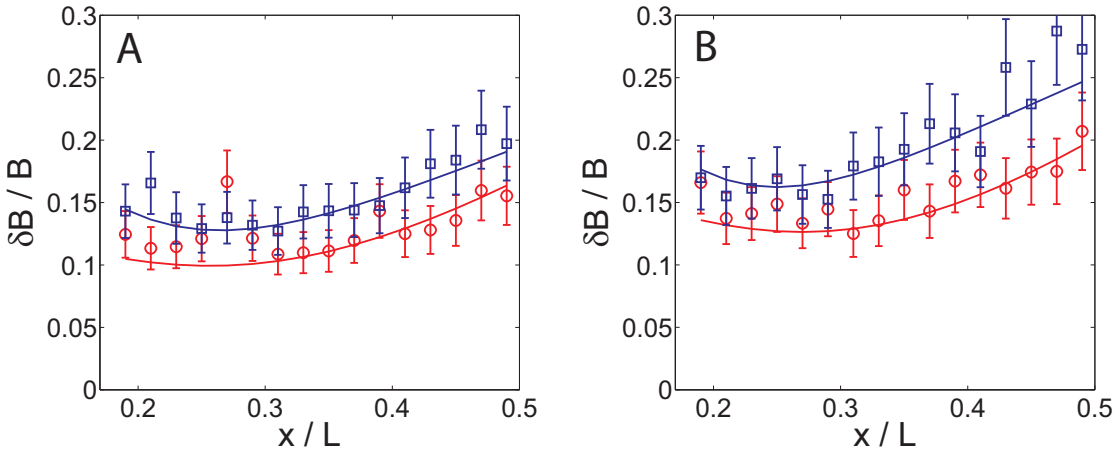


Figure S4: **Coefficient of variation of the observed intensities**. Figure same as Figures 2A and 2B in main paper, except we now plot the relative intensity fluctuations.

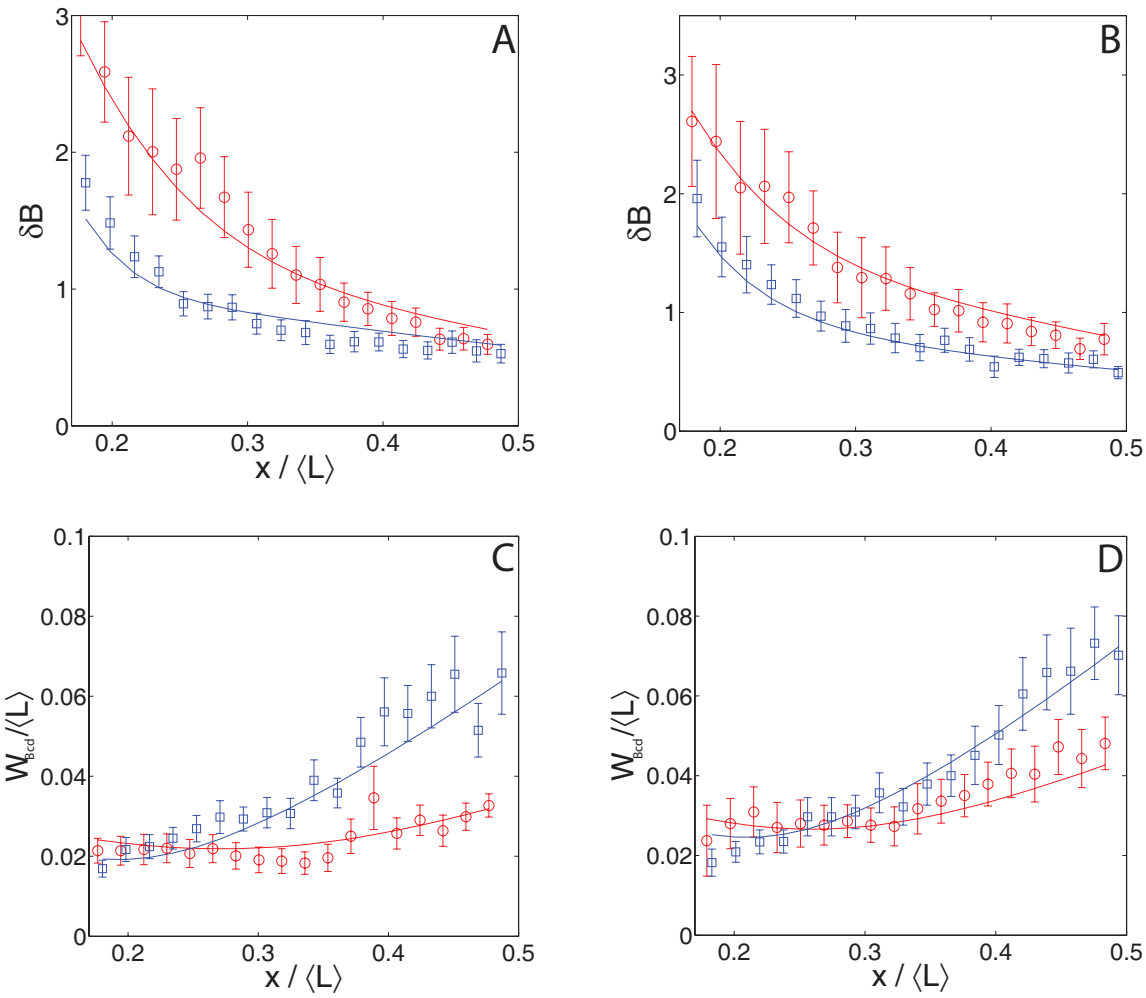


Figure S5: **Fluctuations with respect to absolute position within embryo**. Analysis of the fluctuations in the Bcd gradient, performed using absolute length scales (windows correspond to Fig. 2 of the main paper). Distances are rescaled by the average embryo length to aid comparison with the fully scaled calculation.

| Parameter | Early | Late |
|---|---|---|
| $B_1$ | $19.95 \pm 0.24$ | $15.06 \pm 0.19$ |
| $\Lambda$ | $0.180 \pm 0.002$ | $0.182 \pm 0.002$ |

Table S1: Parameters for fitting wt Bcd intensity data at early and late times.

| Parameter | Early | Late |
|---|---|---|
| $\delta B_1^{ind}/B_1^{ind}$ | $0.060 \pm 0.010$ | $0.086 \pm 0.015$ |
| $\delta\Lambda/\Lambda$ | $0.078 \pm 0.016$ | $0.099 \pm 0.016$ |
| $\alpha_1$ | $-0.80 \pm 0.20$ | $-0.81 \pm 0.23$ |

Table S2: Parameters for fitting observed fluctuations in wt Bcd intensity data at early and late times.

| Parameter | Early | Late |
|---|---|---|
| $a_n$ | $0.902 \pm 0.030$ | $0.783 \pm 0.022$ |
| $y_0$ | $0.391 \pm 0.006$ | $0.398 \pm 0.006$ |

Table S3: Parameters for fitting *nej* embryo Bcd intensity data at early and late times.

| Parameter | Early | Late |
|---|---|---|
| $\delta a_n^{ind}/a_n^{ind}$ | $0.068 \pm 0.017$ | $0.121 \pm 0.013$ |
| $\delta y_0/y_0$ | $0.128 \pm 0.020$ | $0.176 \pm 0.032$ |
| $\alpha_2$ | $1.90 \pm 0.30$ | $2.15 \pm 0.25$ |

Table S4: Parameters for fitting observed fluctuations in *nej* embryo Bcd intensity data at early and late times.

| Parameter | Reference | Value |
|---|---|---|
| $D_0$ | [15] | $0.30\mu m^2 s^{-1} \pm 0.09\mu m^2 s^{-1}$ |
| $k_{3d}$ | [3, 16] | $0.58 \pm 0.07$ |
| $N_{spat}$ | [17] | $36 \pm 6$ |
| $\tau$ | [1, 18, 19] | 10 minutes $\pm$5 minutes |
| $(\Delta x)$ | [17] | $3 \times 10^{-3}\mu m \pm 1 \times 10^{-3}\mu m$ |
| $f_{conv}$ | [17] | $1.2 \pm 0.3$ |

Table S5: Parameters required for computing the positional error $W_{Hb}/L$. Errors on $\Delta x$ and $N_{spat}$ are plausible estimates and not based on direct experimental measurements.

| Parameter | Early | Late |
|---|---|---|
| $\delta B_1^{ind}/B_1^{ind}$ | $0.087 \pm 0.030$ | $0.144 \pm 0.045$ |
| $\delta\Lambda/\Lambda$ | $0.087 \pm 0.022$ | $0.149 \pm 0.034$ |
| $\alpha_1$ | $-0.80 \pm 0.30$ | $-0.40 \pm 0.30$ |
| $\delta a_n^{ind}/a_n^{ind}$ | $0.095 \pm 0.015$ | $0.120 \pm 0.018$ |
| $\delta y_0/y_0$ | $0.157 \pm 0.020$ | $0.222 \pm 0.050$ |
| $\alpha_2$ | $2.2 \pm 0.5$ | $2.3 \pm 0.3$ |

Table S6: Parameters for fitting the observed Bcd intensity fluctuations in wt and *nej* embryos using absolute distances.